



Electrochemical methods for monitoring the performance of a novel Triazole derivative as a corrosion inhibitor in the acidic medium.

M. Boudalia¹, Y. El bakri^{*2}, S. Echihi^{1,3}, A. Harmaoui², J. Sebhaoui², A. Bellaouchou¹, A. Guenbour¹, M. Tabyaoui¹, Y. Ramli⁴, E.M. Essassi²

¹Laboratory of Materials, Nanotechnology and Environment, Faculty of Science, University of Mohamed-V- Av. Ibn Battouta, BP 1014 Agdal-Rabat, Morocco.

²Laboratoire de Chimie Organique Heterocyclique, URAC 21, Pôle de Compétences Pharmacochimie, Université Mohammed V, Faculté des Sciences, Av. Ibn Battouta, BP 1014 Rabat, Morocco

³Laboratory of Water and Environment, Faculty of Sciences of El jadida, BP 20, 24000 El jadida, Morocco

⁴Medicinal Chemistry Laboratory, Faculty of Medicine and Pharmacy, Mohammed V University, 10170 Rabat, Morocco.

Received 04 Jul 2016,

Revised 11 Mar 2017,

Accepted 18 Mar 2017

Keywords

- ✓ Electrochemical measurements
- ✓ EIS
- ✓ Carbon steel;
- ✓ Triazole;
- ✓ Inhibitor.

youness.chimie14@gmail.com
+212677288857

Abstract

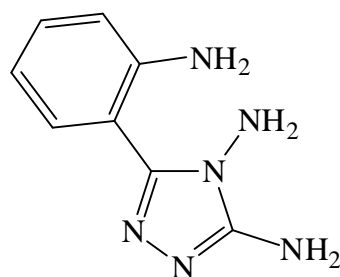
The present investigation includes the study of corrosion inhibition effect of 5-(2-aminophenyl)-4H-3,4-diamine-1,2,4-triazolehydrobromide (ADT) on carbon steel in 1M HCl by electrochemical measurements. The obtained results showed that inhibition efficiency increased with the increasing concentration of inhibitor and decreased with increase in temperature. Potentiodynamic polarization curves indicate that ADT was acting as mixed type of inhibitor. The inhibition efficiency was found to increase with ADT concentration to attain 90% with 10^{-3} M. Langmuir adsorption isotherm model was employed to determine the equilibrium of adsorption for inhibiting process in ADT inhibitor. Nyquist plots revealed that, as the concentration of the inhibitor increases, double layer capacitance (C_{dl}) while charge transfer resistance (R_{ct}) increases. Attempt to correlate the molecular structure to quantum chemical indices was made using density functional theory (DFT).

1. Introduction

Corrosion is a common problem for steel and directly impacts its cost and safety. The corrosion of iron, or rust, can cause structural damage and lead to changes in the mechanical and chemical properties of plants, vessels, pipes, and other processing equipment. These effects demonstrate that corrosion would produce considerable costs if an effective solution is not identified from its study and research. Preventing the corrosion of steel has played an important role in various industries, especially in the chemical and petrochemical processing industries that employ the use of steel. A number of studies have been conducted to investigate effective methods for preventing corrosion. Acids are widely used in industrial processes, such as pickling, cleaning, descaling, etc... Organic compounds containing N, S and O atoms were found to be good corrosion inhibitors of metals [1-11]. The effectiveness of these compounds as corrosion inhibitors has been interpreted in terms of their molecular structure, molecular size, molecular mass, hetero-atoms present and adsorptive tendencies [12]. Under certain conditions, the electronic structure of the organic inhibitors has a key influence on the corrosion inhibition efficiency to the metal. The inhibitors influence the kinetics of the electrochemical reactions which constitute the corrosion process and thereby modify the metal dissolution in acids. A variety of organic compounds have been investigated as corrosion inhibitors [13-15]. A survey of literature reveals that the applicability of organic compounds as corrosion inhibitors for carbon steel in acidic media has been recognized for a long time. Corrosion protection prevents the waste of both resources and money during the industrial

applications and extends the lifetime of the equipment. Triazole possess wide spectrum of activities ranging from anti-bacterial, anti-inflammatory, anticonvulsant, anti-neoplastic [16-19]. A few triazole have been reported as corrosion inhibitors in different corrosive environment [20-22].

In view of the literature cited above, the present work describes the study of inhibitive behavior and adsorption mechanism of 5-(2-aminophenyl)-4H-3,4-diamine-1,2,4-triazole hydrobromide derivative (ADT) was investigated for the inhibition action on the corrosion of Carbon steel in 1M HCl by using electrochemical techniques and quantum chemical calculations. The relationship between calculated quantum chemical parameters and experimental inhibition efficiencies of the inhibitor was discussed. The effect of temperature on the dissolution of Carbon steel in free and inhibited acid solutions has been studied. Various activation and adsorption thermodynamic parameters were calculated and discussed.



Scheme 1: 5-(2-aminophenyl)-4H-3,4-diamine-1,2,4-triazole hydrobromide (ADT).

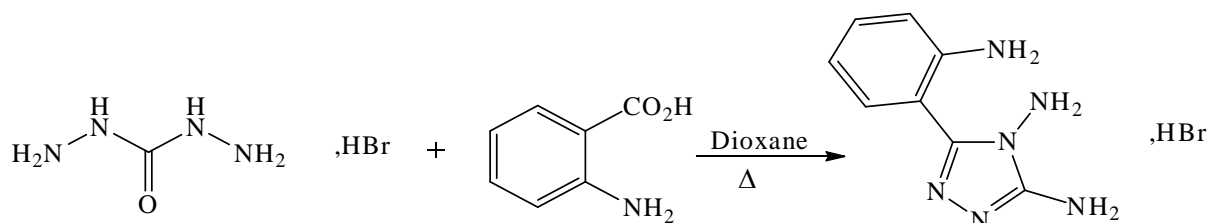
2. Experimental

2.1. Materials

The steel used in this study is a carbon steel (CS) with a chemical composition (in wt%) of 0.370 % C, 0.230 % Si, 0.680 % Mn, 0.016 % S, 0.077 % Cr, 0.011 % Ti, 0.059 % Ni, 0.009 % Co, 0.160 % Cu and the remainder iron Fe. The specimen was used for electrochemical measurements. The exposed surface area was 1cm².

2.2. Synthesis of inhibitor

An equimolar mixture of 1,3-diamino guanidine (0.7g) and anthranilic acid (0.57g) was placed in a 100 ml flask containing 30ml of dioxane and refluxed under continuous stirring for 16 h. After cooling the solution to room temperature, the yellow precipitate formed is filtered and recrystallized from ethanol.



Scheme 2: Characterization of 5-(2-aminophenyl)-4H-1,2,4-triazole-3,4-diamine

The compound was characterized by NMR. ¹H-NMR (DMSO-d₆) (d ppm): 2.95(s,2H,-NH₂),6.54(d,1H,HC=),7.07(dd,1H,HC=),7.28(dd,1H,HC=),8.30(d,1H,HC=). ¹³C-NMR (DMSO-d₆) (d ppm): 147.68(=C-NH₂), 150.16(=C-NH₂), 153.15(C=N), 130.32(HC=), 123.27(-CH), 119.96(-CH), 117.66(-CH), 112.99(C=C).

2.3. Solutions

The aggressive solutions of 1M HCl were prepared by dilution of an analytical grade 37% HCl with double distilled water. The concentration ranges of inhibitor employed was 10⁻⁶-10⁻³M.

3. Electrochemical tests

3.1. Electrochemical impedance spectroscopy

The electrochemical measurements were carried out using Volta lab (Tacussel- Radiometer PGZ 301) potentiostat and controlled by Tacussel corrosion analysis software model (Volta master 4) at under static

condition. The corrosion cell used had three electrodes. The reference electrode was a saturated calomel electrode (SCE). A platinum electrode was used as auxiliary electrode of surface area of 1 cm². The working electrode was carbon steel. All potentials given in this study were referred to this reference electrode. The working electrode was immersed in test solution for 30 min to establish steady state open circuit potential (E_{ocp}). After measuring the E_{ocp}, the electrochemical measurements were performed. All electrochemical tests have been performed in aerated solutions at 303 K. The EIS experiments were conducted in the frequency range with high limit of 100 KHz and different low limit 10 mHz at open circuit potential, with 10 points per decade, at the rest potential, after 30 min of acid immersion, by applying 10mV ac voltage peak-to-peak. Nyquist plots were made from these experiments and the impedance plots are given in the Nyquist representation. Experiments are repeated three times to ensure the reproducibility.

The inhibition efficiency of the inhibitor was calculated from the charge transfer resistance values using the following equation [11].

$$\%IE = \left(1 - \frac{R_{ct}^{\circ}}{R_{ct}}\right) * 100 \quad (1)$$

Where R_{ct}[°] and R_{ct} are the charge transfer resistance in the absence and presence of different concentrations of inhibitor, respectively.

3.2. Potentiodynamic polarization

The electrochemical behavior of carbon steel sample in inhibited and uninhibited solution was studied by recording anodic and cathodic potentiodynamic polarization curves. Measurements were performed in the 1M HCl solution containing different concentrations of the tested inhibitor by changing the electrode potential automatically from -800 to 0 mV versus corrosion potential at a scan rate of 1 mV/s. The linear Tafel segments of anodic and cathodic curves were extrapolated to corrosion potential to obtain corrosion current densities (I_{corr}). From the polarization curves obtained, the corrosion current (I_{corr}) was calculated by curve fitting using the equation (2):

$$I = I_{corr} \left[\exp\left(\frac{2.3 \Delta E}{\beta_a}\right) - \exp\left(\frac{2.3 \Delta E}{\beta_c}\right) \right] \quad (2)$$

The inhibition efficiency was evaluated from the measured I_{corr} values using the relationship:

$$IE\% = \frac{I_{corr}^0 - I_{corr}}{I_{corr}^0} * 100 \quad (3)$$

Where I_{corr}[°] and I_{corr}ⁱ are uninhibited and inhibited corrosion current densities, respectively.

4. Results and Discussion

4.1. Electrochemical impedance spectroscopy

The EIS technique was applied to investigate the electrode/electrolyte interface and corrosion processes that occur on carbon steel surface in presence and absence of 5-(2-aminophenyl)-4H-3,4-diamine-1,2,4-triazole hydrobromide (ADT). To ensure complete characterization of the interface and surface processes, EIS measurements were made at OCP in a wide frequency range at 303 K. Figure 1 shows Nyquist plots for carbon steel electrode immersed in 1M HCl solution at 303 K in absence and presence of various concentrations of ADT at the respective open circuit potential. It is clear from the figure 1 that the diameter of the semicircle increases with the increase in inhibitor concentration in the electrolyte, indicating an increase in corrosion resistance of the material [23].

The value of electrochemical double layer capacitance (C_{dl}) was calculated at the frequency, f_{max} using the following equation [24].

$$C_{dl} = \frac{1}{2\pi f_m R_{ct}} \quad (4)$$

With C_{dl}: Double layer capacitance (μF cm⁻²); f_m: maximum Frequency (Hz) and R_{ct}: Charge transfer resistance (Ω.cm²).

It is observed that addition of inhibitor increases the values of R_{ct} and reduces the C_{dl} values. The decrease in C_{dl} is due to increase in thickness of the electronic double layer [25]. The increase in R_{ct} values is due to the formation of protective film on the metal/solution interface [26,27]. This observation suggests that ADT molecules function by adsorption on metal surface and thereby causing the decrease in C_{dl} values and increase in R_{ct} values. The charge transfer resistance (R_{ct}) values and the interfacial double layer capacitance (C_{dl}) values calculated from the curves are shown in the table 1.

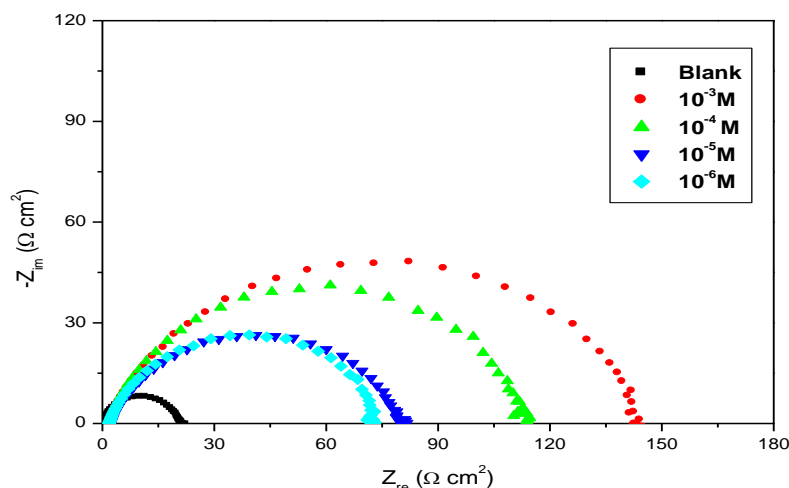


Figure 1. Nyquist plots for C-steel in 1M HCl solution in presence of various concentrations of ADT at 303 K

Table 1. AC impedance data of carbon steel in 1M HCl acid solution at different ADT concentrations at 303 K.

Medium	[C] (M)	R_{ct} ($\Omega \text{ cm}^2$)	C_{dl} ($\mu\text{f/cm}^2$)	f_{max} (Hz)	IE (%)
Blank	1	23.1	200	40	-
ADT	10^{-3}	145	69.5	15.8	84
	10^{-4}	114	88.4	15.8	80
	10^{-5}	80	79.6	25	71
	10^{-6}	73	87.2	25	68

4.2. Potentiodynamic polarization curves

4.2.1. Effect of concentration

The Potentiodynamic polarization curves for CS in 1M HCl solution in the absence and presence of various concentrations of (ADT) at 303 K is shown in figure 2. The extrapolation of Tafel straight line allows the calculation of the corrosion current density (I_{corr}). The values of I_{corr} , the corrosion potential (E_{corr}), cathodic Tafel slopes (β_c) and the percentage of inhibition efficiency (IE %) are given in the table 2.

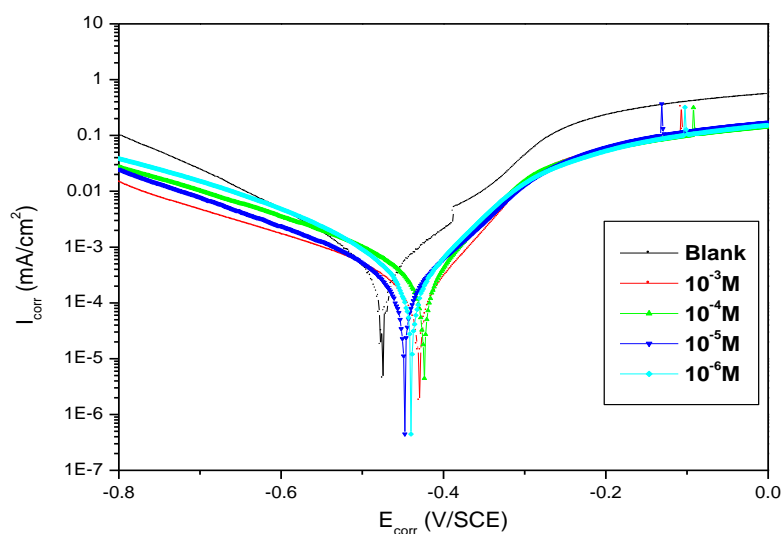


Figure 2. Potentiodynamic polarization curves of CS in 1M HCl at different concentrations of ADT at 303 K.

Table 2. Electrochemical parameters of carbon steel in 1M HCl at different concentrations of ADT.

Medium	[C] (M)	E_{corr} (mV _{SCE})	$-\beta_c$ (mV.dec ⁻¹)	I_{corr} ($\mu\text{A.cm}^{-2}$)	IE (%)
Blank	1	-477	138	579	-
ADT	10^{-6}	-437	157	185	68
	10^{-5}	-445	193	152	74
	10^{-4}	-421	187	123	79
	10^{-3}	-429	177	60	90

It is evident from the figure that cathodic tafel slopes (β_c) remain almost unchanged with increasing inhibitor concentration. This indicates that hydrogen evolution is activation controlled and the addition of inhibitor did not change the mechanism of cathodic hydrogen evolution reaction [28, 29]. It is observed that the inhibition efficiency increased with increasing ADT concentration and exhibited both cathodic and anodic inhibition through adsorption on the CS surface blocking active sites [30]. According to Riggs and others [31,32] if the displacement in $E(i)$ is $> 85\text{mV}$ with respect to E , the inhibitor can be seen as a cathodic or anodic type, (ii) if the displacement in $E(i)$ is < 85 , the inhibitor can be seen as mixed-type. In our study the maximum displacement is less than 85, which indicates that ADT is a mixed-type inhibitor. It is evident from the data that inhibition efficiency (IE %) increases with increase in concentration of the inhibitor. The corrosion current density (I_{corr}) decreases with increase in inhibitor concentration. The maximum inhibition efficiency is 89.6% at 10^{-3}M solution of ADT.

4.2.2. Adsorption isotherm

The adsorption process depends on the structural formula and electronic characteristics of the inhibitor, temperature, the nature of metal surface and the varying degrees of surface-site activity [33, 34]. In actual fact, the H_2O molecules could be adsorbed at the electrode/solution interface. To this effect, the adsorption of organic inhibitor molecules can be considered as a quasi-substitution process between the organic compounds in the aqueous phase $\text{Org}(\text{sol})$ and water molecules at the electrode surface $\text{H}_2\text{O}(\text{ads})$ [35]:



Where (n) is the size ratio, that is the number of water molecules replaced by one organic inhibitor.

The efficiency of a corrosion inhibitor mainly depends on its adsorption ability on the metal surface. So, it is necessary to know the mechanism of adsorption and the adsorption isotherm that can give valuable information on the interaction of inhibitor and metal surface. The surface protection of CS depends upon how the inhibitor molecule will adsorbed on the metal surface and also ionization and polarization of molecules [36]. The degree of surface coverage (θ) as function of concentration (C) of the inhibitor was studied graphically by 1M HCl medium. According to this adsorption isotherm, θ is related to the inhibitor concentration, C, and adsorption equilibrium constant K_{ads} through the following expression (5):

$$\frac{\theta}{1-\theta} = C \cdot K_{\text{ads}} \quad (5)$$

By rearranging this equation (6):

$$C \cdot K_{\text{ads}} = \frac{\theta}{1-\theta} \quad (6)$$

Where K_{ads} is the adsorption/desorption equilibrium constant, C_{inh} is the corrosion inhibitor concentration in the solution.

The surface coverage was tested graphically by fitting a suitable adsorption isotherm. In the present case, the plots of C/θ versus C (Figure 3) yields straight lines with the linear correlation coefficient (R^2) values close to unity, which suggests that the adsorption of ADT in 1M HCl medium on carbon steel surface obeys the Langmuir adsorption isotherm. The slope of this line was (1.10). The thermodynamic parameters for the corrosion of carbon steel in 1M HCl acid in the presence and absence of different concentrations of ADT is given in the Table 3. The free energy of adsorption ΔG_{ads}^0 can be calculated from the K_{ads} value obtained from the above correlation:

$$\Delta G_{\text{ads}}^0 = -RT \ln(K_{\text{ads}} \cdot 55.5) \quad (7)$$

Where 55.5 is the concentration of water, $R = 8.314 \text{ J.K}^{-1}.\text{mol}^{-1}$ is the universal gas constant and T is the absolute temperature (K), K_{ads} the adsorption/desorption equilibrium constant.

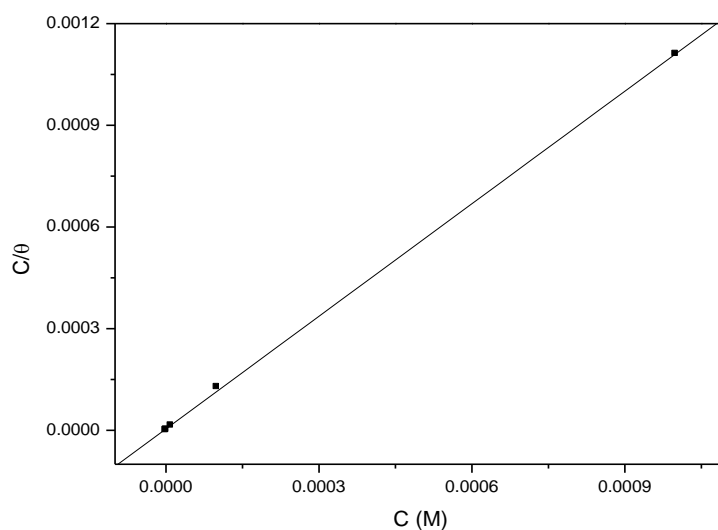


Figure 3: Langmuir adsorption isotherm of ADT on the carbon steel surface in HCl solution

Table 3: Thermodynamic parameters for the corrosion of carbon steel in 1M HCl in the absence and presence of ADT.

Inhibitor	R ²	Slope	K (M ⁻¹)	ΔG _{ads} [°] (kJ mol ⁻¹)
ADT	0.99788	1.10	223001.4	-41.2

The ΔG_{ads}° values are also presented in Table 4, the negative sign of ΔG_{ads}° indicates the spontaneity of the adsorption process and stability of the adsorbed film on the electrode surface [37]. Furthermore, values of ΔG_{ads}° up to -20 kJ mol^{-1} are reliable with the electrostatic interaction between the charged molecules and the charged metal (physisorption) while those more negative than -40 kJ mol^{-1} involve sharing or transfer of electrons from the inhibitor molecules to the metal surface to form a co-ordinate type of bond (chemisorption) [38]. Accordingly, the value of $\Delta G_{ads}^{\circ} = -41.2 \text{ kJ/mol}$ we propose chemisorption of ADT molecules on the carbon steel surface. In fact, because of strong adsorption of H_2O molecules on the surface of steel, it may be assumed that removal of water molecules from the surface is accompanied by chemical interaction between the metal surface and the formed film [39].

4.2.3. Effect of temperature

Figure 4 and 5 shows the effect of temperature on the corrosion behavior of carbon steel using polarization methods at temperature range 303-333K in the absence and the presence of ADT in 1MHCl.

From Table 4, the studied compound demonstrated decreased in the inhibition efficiency (IE %) at higher temperature. The results for IE% differ slightly at certain temperature for the inhibitor, but sustain the efficiency to protect carbon steel from corroded in the acid solution at highest temperature studied compared to the blank of 1M HCl. The inhibition efficiencies were found to decrease with increasing temperature from 303-333 K. Desorption of inhibitor is aided by increasing temperature. This proves that the inhibition occurs through the adsorption of the inhibitor on the metal surface. The corrosion current density increases with the rise of temperature and markedly pronounced in the absence of inhibitor. The activation parameters for the corrosion process were calculated from the Arrhenius type plot according to the following equation (8):

$$I_{corr} = A \exp\left(-\frac{E_a}{RT}\right) \quad (8)$$

Where E_a is the activation energy of the corrosion process, is the Arrhenius pre-exponential factor, T is the absolute temperature, and R is the universal gas constant.

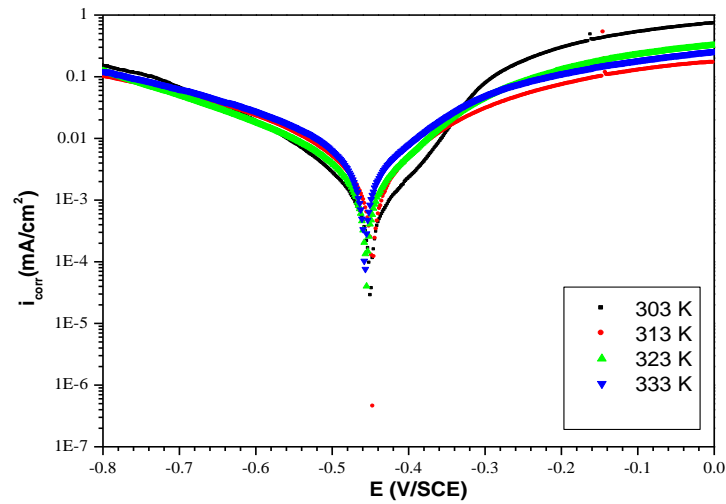


Figure 4: Polarization curves for steel in 1M HCl at different temperatures

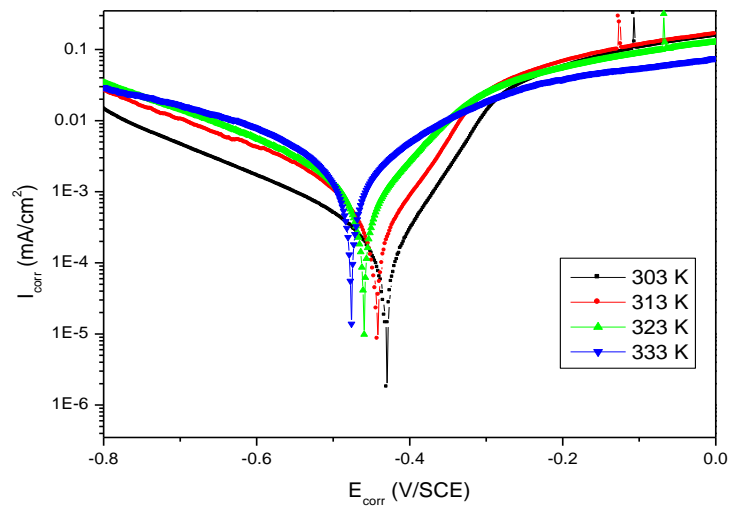


Figure 5 : Polarization curves for steel in 1M HCl + 10^{-3} M ADT at different temperatures.

Table 4: various corrosion parameters for carbon steel in 1M HCl in absence and presence of optimum concentration of ADT at different temperatures.

Temp (K)	I_{corr} ($\mu\text{A}/\text{cm}^2$)		θ	IE (%)
	Blank	ADT		
303	579	60	0.89	89
313	694	132	0.80	80
323	2026	420	0.79	79
333	2102	487	0.76	76

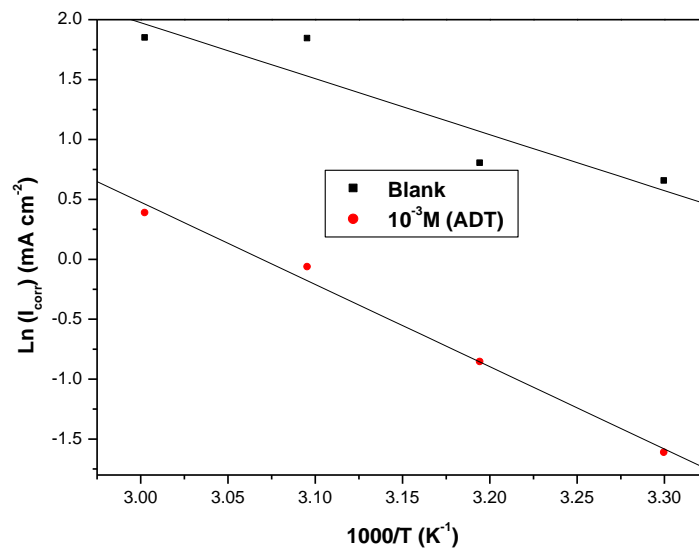


Figure 6: Arrhenius plots of C-steel in 1M HCl with and without 10⁻³M of ADT

The values of E_a for CS in 1M HCl without and with various concentrations of inhibitor are obtained from the slope of the plot of $\text{Ln } I_{\text{corr}}$ versus $1/T$ and are shown in Table 5. E_a values for inhibited systems are higher than those for the uninhibited systems suggest that dissolution of carbon steel is slow [40]. This means the presence of the inhibitor induces an energy barrier for corrosion reaction and the barrier increases with increasing concentration. At higher temperatures, there is an appreciable decrease in the adsorption of the inhibitor on the metal surface and a corresponding rise in the corrosion rate occurred.

Figure 7 shows the Alternative Arrhenius plots of $\text{Ln } (I_{\text{corr}}/T)$ versus $1/T$ for carbon steel dissolution in HCl medium in the absence and presence of different concentrations of ADT was used to calculate the values of activation thermodynamic parameters such as enthalpy of activation (ΔH_a) and entropy of activation (ΔS_a) using the following relation:

$$I_{\text{corr}} = \frac{RT}{Nh} \exp\left(\frac{\Delta S_a^\circ}{R}\right) \exp\left(-\frac{\Delta H_a^\circ}{RT}\right) \quad (9)$$

The values of E_a and, ΔH_a and, ΔS_a were estimated from the slopes of the straight lines and given in Table 5.

Where E_a is the activation energy of the corrosion process, A is the pre-exponential factor, R the general gas constant, h is the plank's constant, N is Avogadro's number, ΔS_a is the apparent entropy of activation and ΔH_a is the apparent enthalpy of activation.

From figure 7, the straight lines are obtained with a slope $\left(\frac{-\Delta H_a}{RT}\right)$ and an intercept of $\text{Ln}(R/Nh) + (\Delta S_a/R)$ from which the values of ΔH_a and ΔS_a are calculated and are given in Table 5. The apparent activation energy (E_a) at optimum concentration of 5-(2-aminophenyl)-4H-3,4-diamine1,2,4-triazole hydrobromide (ADT), was determined by linear regression between $\text{Ln } I_{\text{corr}}$ and $1/T$ (Figure 5) and the results is shown in Table 5. The linear regression coefficient was close to 1, indicating that the steel corrosion in hydrochloric acid can be elucidated using the kinetic model. Inspection of Table 5 showed that the value of E_a determined in 1M HCl containing our compound is higher (59.74 kJ mol⁻¹) for ADT than that for uninhibited solution (40.12 KJ.mol⁻¹). Szauer and Brand explained that the increase in activation energy can be attributed to an appreciable decrease in the adsorption of the inhibitor on the steel surface with increase in temperature. As adsorption decreases more desorption of inhibitor molecules occurs because these two opposite processes are in equilibrium. Due to more desorption of inhibitor molecules at higher temperatures the greater surface area of steel comes in contact with aggressive environment, resulting increased corrosion rates with increase in temperature [41]. The positive shift of enthalpy of activation (ΔH_a) with the presence of inhibitor concentration reflects that the process of adsorption of the inhibitor on the CS surface is an endothermic process [42], and the negative values of entropy

of activation (ΔS_a) represents association rather than dissociation of inhibitor indicating the decrease of system disorder due to the adsorption of inhibitor molecules on the c-steel surface [43–45]. The value of ΔS_a is higher for inhibited solutions than the uninhibited solution reflecting an increase in randomness on going from reactants to the activated complex. The increase in values of ΔS_a by the adsorption of inhibitor molecules on the carbon steel surface could be regarded as quasi substitution between the inhibitor molecules in the aqueous phase and water molecules on electrode surface [46]. In such condition, the adsorption of inhibitor molecules follow desorption of water molecules from the electrode surface and hence decrease the electrical capacity of carbon steel.

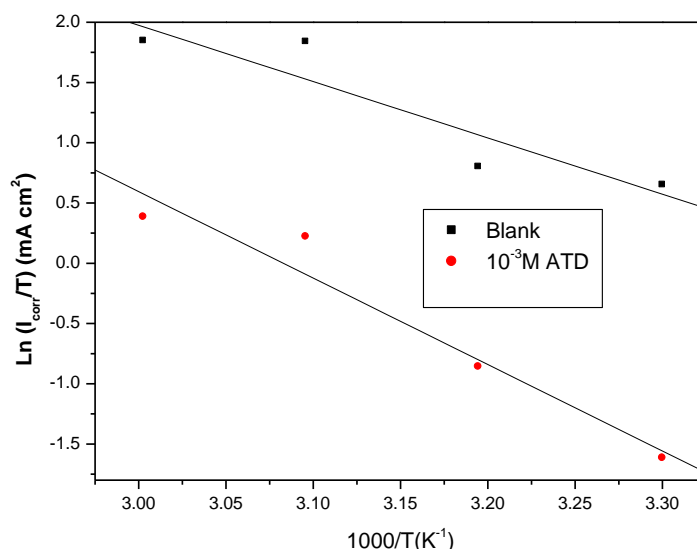


Figure 7: Arrhenius plots of $\text{Ln } I_{\text{corr}}/T$ vs. $1/T$ for steel in 1M HCl in the absence and the presence of ADT at optimum concentration.

Table 5: Activation parameters for the steel dissolution in 1M HCl in the absence and the presence of ADT at optimum concentration.

Medium	Linear regression coefficient (r)	E_a (kJ/mol)	ΔH_a (kJ mol ⁻¹)	ΔS_a (J mol ⁻¹ K ⁻¹)
1M HCl	0.99925	40.12	38.84	-64.59
ADT	0.99984	59.74	57.10	-22.26

5. Scanning electron microscopy

Figure 8 shows a SEM photograph recorded for C-steel samples exposed in 1M HCl solution without figure (a) and with 10^{-3} M of ADT for 6 h at 303K (b). The SEM micrographs of the corroded carbon steel in the presence of 1 M HCl solution are shown in Figure (8a). The faceting seen in this figures was a result of pits formed due to the exposure of carbon steel to the acid. The influence of the inhibitor addition 10^{-3} M of ADT on the carbon steel in 1 M HCl solution is shown in Figure (8b).

The morphology in figure (8b) shows a rough surface, characteristic of uniform corrosion of C-steel in acidic medium, as previously reported, that corrosion does not occur in presence of inhibitor and hence corrosion was inhibited strongly when the inhibitor was present in the hydrochloric, and the surface layer is very rough. In contrast, in the presence of 10^{-3} M of ADT, there is much less damage on the steel surface, which further

confirms the inhibition action. Also, there is an adsorbed film on carbon steel surface (Figure (8b)). In accordance, it might be concluded that the adsorption film can efficiently inhibit the corrosion of carbon steel.

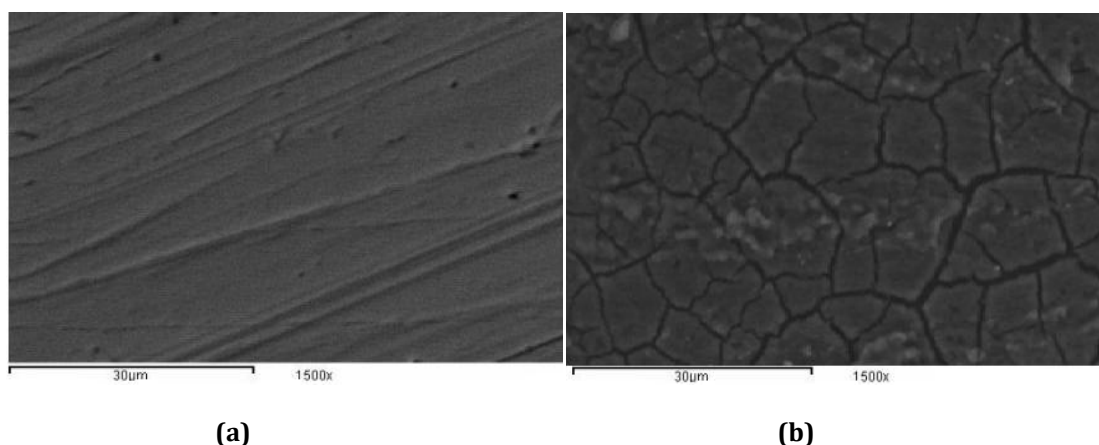


Figure 8: SEM micrograph of carbon steel surface (a) in the absence of ADT (b) in the presence of ADT

Conclusions

- The synthesized of 5-(2-aminophenyl)-4H-3,4-diamine-1,2,4-triazole hydrobromide showed good inhibition efficiency for the corrosion of carbon steel in 1M HCl solution and the inhibition efficiency was found to increase with increasing concentration of the inhibitor.
- Both polarization and electrochemical impedance data have shown increased inhibition efficiency with respect to increase in the concentration of inhibitor. All the concentration has exhibited the good IE% and the maximum inhibition efficiency is 90% at 10^{-3} M solution of ADT.
- Langmuir adsorption isotherm model was employed to determine the equilibrium of adsorption for inhibiting process in ADT inhibitor.
- SEM micrograph confirmed the absence of corrosion product on the metal surface in the presence of inhibitor. These studies reveal that ADT act as good inhibitor at different concentration

References

1. Badr G. E., *Corros. Sci.* 51 (2009) 2529.
2. Ren Y., Luo Y., K. Zhang, Zhu G., Tan X., *Corros. Sci.* 50 (2008) 3147.
3. Jacob K. S., Parameswaran G., *Corros. Sci.* 52 (2010) 228.
4. Abd El-Maksoud S. A., Fouda A. S., *Mater ChemPhys* 93 (2005) 84.
5. Singh A. K., Quraishi M. A., Ebenso E.E., *Int. J. Electrochem. Sci* 6 (2011) 5688.
6. Behpour M., Ghoreishi S.M., Soltani N., Salavati-Niasari M., Hamadani M., Gandomi A., *Corros. Sci.* 50 (2008) 2181.
7. Ismaily Alaoui K., El Hajjaji F., Azaroual M.A., Taleb M., Chetouani A., Hammouti B., Abridgach F., Khoutoul M., Abboud Y., Aouniti A., Touzani R., *J. Chem. Pharmac. Res.*, 6 N°7 (2014) 63-81
8. Singh A. K., Quraishi M. A., *Corros. Sci.* 52 (2010) 160.
9. Zarrouk A., Zarrok H., Salghi R., Hammouti B., Al-Deyab S.S., Touzani R., Bouachrine M., Warad I., Hadda T. B., *Int. J. Electrochem. Sci.*, 7 N°7 (2012) 6353-6364
10. Asan A., Soylu S., Kiyak T., Yildirim F., Oztas S. G., Ancin N., Kabasakaloglu M., *Corros. Sci.* 48 (2006) 3944.
11. Harmaoui A., El Fal M., Boudalia M., Tabyaoui M., Guenbour A., Bellaouchou A., Ramli Y., Essassi E. M., *J. Mater. Environ. Sci.* 6 (9) (2015) 2519.
12. Aljourani J., Raeissi K., Golozar M. A., *Corros. Sci.* 51 (2009) 1843
13. Zarrouk A., Warad I., Hammouti B., Dafali A., Al-Deyab S.S., Benchat N., *Int. J. Electrochem. Sci.* 5 (2010) 1516.

14. Boudalia M., Bellaouchou A., Guenbour A., Tabiyaoui M., El Fal M., Ramli Y., Essassi E.M., Elmsellem H., Hammouti B., *Mor. J. Chem.* 2 N°2 (2014) 109.
15. Larif M., Elmidaoui A., Zarrouk A., Zarrok H., Salghi R., Hammouti B., Oudda H., Bentiss F., *Res. Chem. Intermed.*, 2012 DOI 10.1007/s11164-012-0788-2.
16. Ashok M., Holla B.S., *J. Pharmacol. Toxicol.* 2 (2007) 256.
17. Hosur M.C., Talwar M.B., Bennur R.S., Benur S.C., Patil P.A., Sambrekar S., *Indian J. Pharm.Sci.* 55 (1993) 86.
18. Holla B.S., Veerendra B., Shivananda M.K., Poojary B., *Eur. J. Med. Chem.* 38, (2003) 759.
19. Prasad D.J., Ashok M., Karegoudar P., Poojary B., Holla B.S., Sucheta K.N., *Eur. J. Med. Chem.* 44, (2009) 551.
20. Finsgar M., Milosev I., *Corros. Sci.* 52 (2010) 2737
21. Sherif E.M., Park Su-M., *Electrochim. Acta.* 51 (2006) 4665
22. Amin M.A., Abd El-Rehim S.S., El-Sherbini E.E.F., Bayyomi R.S., *Electrochim. Acta* 52 (2007) 3588.
23. Ghareba S., Omanovic S., *Corros. Sci.*, 52 (2010) 2104.
24. Kharbach Y., Haoudi A., Skalli M.K., Kandri Rodi Y., Aouniti A., Hammouti B., Senhaji O., Zarrouk A., *J. Mater. Environ. Sci.* 6 (10) (2015) 2906-2916
25. Boudalia M., Sebbar N.K., Lahmidi S., Ouzidan Y., Essassi E. M, Tayebi H., Bellaouchou A., Guenbour A., Zarrouk A., *J. Mater. Environ. Sci.* 7 (3) (2016) 878.
26. Murlidharan S., Phani K.L.N., Pitchumani S., Ravichandran S., *J. Electrochem. Soc.*, 142 (1995)1478.
27. ElHajjaji F., Greche H., Taleb M., Chetouani A., Aouniti A., Hammouti B., *J. Mater. Environ. Sci.* 7 (2) (2016) 566-578.
28. Ateya B. G., El-Khair M.B.A., Abdel-Hamed I.A., *Corros. Sci.*, 16 (1976) 163.
29. El Bakri Y., Boudalia M., Echihi S., Harmaoui A., Sebhaoui J., Elmsellem H., Ben Ali A., Ramli Y., Guenbour A., Bellaouchou A., Essassi E.M., *J. Mater. Environ. Sci.* 8(2) (2017) 388.
30. Ferreira E. S., Giancomlli C., Giacomlli F. C., Spinelli A., *Mater. Chem. Phys.* 83 (2004) 129.
31. Riggs Jr. O.L., Corrosion Inhibition, second ed., C.C. Nathan, Houston, TX, 17 (1973) 46.
32. Quraishi M.A., Ahmad S., Venkatachari G., *Bull. Electrochem.*, 12 (1996) 137.
33. El-Awady A., Abd-El-Nabey A.B., Aziz S.G., *J. Electrochem. Soc.* 139 (1992) 2149.
34. Bockris J.O.M., Reddy A.K.N, Modern Electrochemistry, Plenum Pub. Corp. New York, 2 (1976) 2437.
35. Wang X., Yang H., Wang F., *Corros. Sci.* 52 (2010) 1268.
36. Refaey S.A.M., Taha F., Abd El-Malak A. M., "Corrosion and inhibition of 316 L stainless steel in neutral medium by 2- mercaptobenzimidazole," *International Journal of Electrochemical Science*, 1 (2006) 19.
37. Anejjar A., Salghi R., Zarrouk A., Zarrok H., Benali O., Hammouti B., Al-Deyab S.S., Benchat N-E., Saddik R., DOI10.1007/s11164-013-1244-7, *Res. Chem. Intermed.* 41 (2015) 913.
38. Hussin M.H., Kassim M., *Mater. Chem. Phys.* 125 (2011) 461.
39. Elmsellem H., Harit T., Aouniti A., Malek F., Riahi A., Chetouani A., Hammouti B., *Protection of Metals and Physical Chemistry of Surfaces*, 2015, 51(5), 884
40. Poornima T., Nayak J., Shetty A.N., "Corrosion inhibition of the annealed 18 Ni 250 grade maraging steel in 0. 67 M phosphoric acid by 3, 4-dimethoxybenzaldehydethiosemicarbazone," *Chemical Sciences Journal.* 69 (2012) 14.
41. Szauer T., Brand A., *Electrochim. Acta.* 26 (1981) 1219.
42. Abdallah M., Helal E.A., Fouda A.S., "Aminopyrimidine derivatives as inhibitors for corrosion of 1018 carbon steel in nitric acid solution," *Corros. Sci.* 48 (2006) 1654.
43. Abd El-Rehim S.S., Refaey S.A. M., Taha F., Saleh M.B., Ahmed R.A., "Corrosion inhibition of mild steel in acidic medium using 2-amino thiophenol and 2-cyanomethyl benzothiazole," *J. Appl. Electrochem.* 31 (2001) 435.
44. Yurt A., Balaban A., Kandemir S.U., Bereket G., Erk B., "Investigation on some Schiff bases as HCl corrosion inhibitors for carbon steel," *Materials Chemistry and Physics.* 85 (2004) 426.
45. Tang L., Li X., Si Y., Mu G., Liu G., *Materials Chemistry and Physics.* 95 (2006) 38.
46. Bhattacharya A.K., Naiya T.K., Mandal S.N., Das S.K., "Adsorption, kinetics and equilibrium studies on removal of Cr(VI) from aqueous solutions using different low-cost adsorbents," *Chemical Engineering Journal.* 137 (2008) 541.

(2017) ; <http://www.jmaterenvironsci.com>